

J/ψ Gluonic Dissociation Revisited : II. Hydrodynamic Expansion Effects

B. K. Patra¹ and V. J. Menon²

¹ Dept. of Physics, Indian Institute of Technology, Roorkee 247 667, India

² Dept. of Physics, Banaras Hindu University, Varanasi 221 005, India

Abstract

We explicitly take into account the effect of hydrodynamic expansion profile on the gluonic breakup of J/ψ 's produced in an equilibrating parton plasma. Attention is paid to the space-time inhomogeneities as well as Lorentz frames while deriving new expressions for the gluon number density n_g , average dissociation rate $\langle\tilde{\Gamma}\rangle$, and ψ survival probability S . A novel type of partial wave *interference* mechanism is found to operate in the formula of $\langle\tilde{\Gamma}\rangle$. Nonrelativistic longitudinal expansion from small length of the initial cylinder is found to push the $S(p_T)$ graph above the no flow case considered by us earlier [9]. However, relativistic flow corresponding to large length of the initial cylinder pushes the curve of $S(p_T)$ downwards at LHC but upwards at RHIC. This mutually different effect on $S(p_T)$ may be attributed to the different initial temperatures generated at LHC and RHIC.

PACS numbers: 12.38M

I INTRODUCTION

Extensive literature exists on the possible suppression [1]- [6] of the J/ψ mesons in a quark-gluon plasma and their proposed regeneration [7]. Among the well known mechanisms of J/ψ dissociation the one due to gluonic bombardment [8] deserves special attention here. Recently the present authors [9] considered the statistical mechanics of important physical observables *viz.* the gluon number density, thermally-averaged $g - \psi$ break-up rate, and the ψ meson survival probability appropriate to RHIC/LHC initial conditions. We found [9] that these observables are *significantly* affected if one employs improved expressions for the gluon distribution function, $g - \psi$ relative flux, and ψ meson formation time.

Of course, it is a well-recognized fact that the longitudinal/transverse expansion of the medium controls the master rate equations [10] for the time-evolution of the plasma temperature and parton fugacities. But the literature *does not* tell how the fluid velocity profile itself influences the Lorentz transformations connecting the rest frames of the fireball, plasma, and ψ meson. In other words, since the *flow velocity profile* causes inhomogeneities in space-time, hence the scenario of J/ψ gluonic break-up may be affected in a quite nontrivial manner and the aim of the present paper is to address this hitherto unsolved problem.

Sec.II below recalls a few aspects of relativistic hydrodynamics for the sake of ready reference. Next, a new expression for the gluon number density is derived in Sec.III showing how an extra dilation factor γ associated with the flow appears. Next, in Sec.IV careful Lorentz transformations are used to calculate the flux-weighted cross section and explicit dependence is brought out on the hydrodynamic velocity \vec{w} observed in J/ψ rest frame. Next, Sec.V develops the machinery for computing the J/ψ survival probability as a function of transverse momentum. Finally, Sec.VI summarizes our main conclusions applicable to nonrelativistic/relativistic flows.

II ASPECTS OF HYDRODYNAMICS

Preliminaries: Consider the rest frame of the hot, dense fireball produced in ultrarelativistic heavy ion collision. Within an initial time span $t_i = \tau_0 \sim 0.5$ fm/c it is supposed to achieve local thermal equilibrium. The plasma now expands rapidly, gets cooled at

the expense of internal energy, and is driven towards chemical equilibration through partonic reactions. The plasma's life ends, i.e., freeze-out occurs at the instant t_{life} when the temperature drops to 200 MeV, say. Such a picture of collective flow is known to have profound effect on the measured dilepton spectrum [11], dependence of colour screening mechanism on equation of state [12], anisotropy in the transverse-momentum distribution [13] of output hadrons, azimuthal asymmetry of J/ψ suppression in noncentral heavy-ion collisions [14], etc.

Equation of motion: We employ the units $\hbar = c = 1$ and follow closely the hydrodynamic summary given by Pal et al [12] based upon *cylindrical symmetry* appropriate to central collisions. In the fireball frame a general time-space point x and the fluid 4 velocity u have the form

$$\begin{aligned} x &= (t, \vec{x}) ; u = (\gamma, \gamma\vec{v}) \\ \gamma &= (1 + \vec{v}^2)^{1/2} = (1 - \vec{v}^2)^{-1/2} \end{aligned} \quad (1)$$

where \vec{v} is the local 3 velocity and γ is the corresponding Lorentz factor. Ignoring viscosity the conservation law for the energy- momentum tensor $T^{\mu\nu}$ reads

$$\partial_\mu T^{\mu\nu} = 0 ; T^{\mu\nu}(x) = (\epsilon + P)u^\mu u^\nu + Pg^{\mu\nu} \quad (2)$$

where the energy density ϵ and pressure P are supposed to be measured in a frame comoving with the plasma. The relationship between *the fireball usual time t and medium proper time τ* is, of course

$$\frac{d\tau}{dt} = \frac{1}{\gamma} ; t_i \leq t \leq t_{\text{life}} \quad (3)$$

Longitudinal Expansion: In Bjorken's boost-invariant, one-dimensional flow the profile admits a simple *analytical* solution

$$\vec{v} = \frac{z}{t}\hat{e}_z ; \tau = (t^2 - z^2)^{1/2} \geq \tau_0 \quad (4)$$

where \hat{e}_z is a unit vector along the collision axis. The corresponding temperature $T \propto \tau^{-1/3}$ is known to fall rather slowly, *e.g.* in the case of gold nuclei colliding at RHIC. Hence the J/ψ suppression remains comparatively high *via* the colour screening/gluonic dissociation mechanisms.

Transverse Expansion: As summarized in Refs. [12]-[11] the 4-velocity profile becomes quite intricate and a numerical integration of the dynamical equations (2,3) becomes very hard in the case of 3 + 1 dimensional expansion. For our purpose it will

suffice to assume that the collective flow occurs only along the lateral directions without rotation as given by the *empirical* ansatz

$$\vec{v} = \frac{r}{t} \hat{e}_r ; \tau = (t^2 - r^2)^{1/2} \quad (5)$$

where \hat{e}_r is the unit vector along \vec{r} in a cylindrical coordinate system (r, z, ϕ) . It is known from numerical solution of (2) that transverse flow causes very rapid cooling in the case of lead nuclei colliding at LHC. Hence the J/ψ survival chance becomes relatively high *via* the colour screening/gluonic dissociation scenarios. We now proceed to formulate the statistical mechanics of some physical observables following closely the logic of Ref.[9].

III GLUON NUMBER DENSITY

Preliminaries: Working in the fireball rest frame and assuming local thermal equilibrium let the symbol x denote a typical time-space point, u the medium 4- velocity, T the absolute temperature, $K = (K^0, \vec{K})$ the gluon 4-momentum, 16 the spin-colour degeneracy factor, λ_g the gluon fugacity, f the one-body Bose-Einstein distribution function, and n_g the gluon number density given mathematically by

$$f = \frac{\lambda_g}{e^{K \cdot u/T} - \lambda_g} ; n_g(x) = 16 \int \frac{d^3 \vec{K}}{(2\pi)^3} f \quad (6)$$

It may be noted that generally $\lambda_g < 1$ for chemically unequilibrated plasma and $K \cdot u$ is tedious in the fireball frame.

Comoving Frame: If $k = (k^0, \vec{k})$ is the gluon 4-momentum in the local rest frame of the plasma then by Lorentz transformations

$$K \cdot u = k^0 ; K^0/k^0 = \gamma(1 + \vec{v} \cdot \hat{k}) \quad (7)$$

where γ, \vec{v} refer to the fluid motion of (1) and \hat{k} is a unit vector along \vec{k} . Substitution into (6) simplifies the distribution function as

$$f = \frac{\lambda_g}{e^{k^0/T} - \lambda_g} = \sum_{n=1}^{\infty} \lambda_g^n e^{-nk^0/T} \quad (8)$$

Also, upon taking the polar axis for integration along \hat{v} and writing $\vec{v} \cdot \hat{k} = |\vec{v}| \cos \theta_{kv}$ our number density reduces to

$$n_g(x) = 16 \int \frac{d^3 k}{(2\pi)^3} \frac{K^0}{k^0} f \quad (9)$$

$$= \frac{2}{\pi^3} \int_0^\infty dk^0 k^{02} \int_{-1}^1 d \cos \theta_{kv} \int_0^{2\pi} d\phi_{kv} \gamma (1 + |\vec{v}| \cos \theta_{kv}) \sum_{n=1}^\infty \lambda_g^n e^{-nk^0/T} \quad (10)$$

$$= \frac{16}{\pi^2} \gamma T^3 \sum_{n=1}^\infty \frac{\lambda_g^n}{n^3} \quad (11)$$

Remarks: This result is *new* and shows in a compact manner how the number density depends upon γ , T , and λ_g (although these dependences are generally interwoven through the evolution equations). It may be stressed that inspite of the occurrence of a $\vec{v} \cdot \hat{k}$ term in (7) our final n_g depends on \vec{v}^2 through γ . Our (11) generalizes an earlier expression obtained by Xu et al [8] who ignored the flow velocity \vec{v} completely and worked with a factorized form of the Bose-Einstein distribution containing λ_g only in the numerator.

Numerical Estimate at t_i : The behaviour of (11) can be easily studied at the instant when the thermalized fireball was formed in high energy heavy ion collision. The initial conditions predicted by HIJING Monte Carlo simulations are summarized in Table 1.

Table 1: Initial values for the time, temperature, fugacities etc. at RHIC(1), LHC(1) only [15]

	$T(\text{GeV})$	$t_i = \tau_0$ (fm)	λ_g	λ_q	$n_g^{v=0.1c}(\text{fm})^{-3}$	$n_g^{v=0.9c}(\text{fm})^{-3}$
RHIC(1)	0.55	0.70	0.05	0.008	1.78	4.05
LHC(1)	0.82	0.5	0.124	0.02	14.73	33.63

There the gluon densities computed *via* (11) in the nonrelativistic ($v \approx 0.1c$) and ultrarelativistic ($v \approx 0.9c$) regions are also listed showing a relative enhancement by the factor

$$\frac{n_{gi}^{v=0.9c}}{n_{gi}^{v=0.1c}} \approx \frac{(1 - 0.01)^{1/2}}{(1 - 0.81)^{1/2}} \approx 2.28 \quad (12)$$

Temporal Evolution: It is very tedious to employ the exact distribution function f of (6) for determining how the fugacities and temperature evolve with the proper time τ of the medium. Hence we shall directly borrow the master rate equations from existing literature based upon approximately *factorized* form of f . It is plausible to assume that such an approximation will not markedly affect our final conclusions since

$\lambda_g < 1$. For longitudinal expansion parametrized by (4) the relevant ordinary differential equations [10] are known to be

$$\begin{aligned}\frac{\dot{\lambda}_g}{\lambda_g} + 3\frac{\dot{T}}{T} + \frac{1}{\tau} &= R_3(1 - \lambda_g) - 2R_2\left(1 - \frac{\lambda_g^2}{\lambda_q^2}\right), \\ \frac{\dot{\lambda}_q}{\lambda_q} + 3\frac{\dot{T}}{T} + \frac{1}{\tau} &= R_2\frac{a_1}{b_1}\left(\frac{\lambda_g}{\lambda_q} - \frac{\lambda_q}{\lambda_g}\right), \\ \left(\lambda_g + \frac{b_2}{a_2}\lambda_q\right)^{3/4} T^3 \tau &= \text{const}\end{aligned}\tag{13}$$

Here $\lambda_q(\lambda_g)$ is the quark (gluon) fugacity, N_f the number of flavours, and remaining symbols are defined by

$$\begin{aligned}R_2 &= 0.5n_g\langle v\sigma_{gg\rightarrow q\bar{q}}\rangle, & R_3 &= 0.5n_g\langle v\sigma_{gg\rightarrow ggg}\rangle \\ a_1 &= 16\zeta(3)/\pi^2, & a_2 &= 8\pi^2/15 \\ b_1 &= 9\zeta(3)N_f/\pi^2, & b_2 &= 7\pi^2N_f/20\end{aligned}\tag{14}$$

Next, for transverse expansion parametrized by (5) the appropriate partial differential equations [12] read

$$\partial_\tau T^{00} + r^{-1}\partial_r(rT^{01}) + \tau^{-1}(T^{00} + P) = 0\tag{15}$$

and

$$\partial_\tau T^{01} + r^{-1}\partial_r[r(T^{00} + P)v_r^2] + \tau^{-1}T^{01} + \partial_r P = 0\tag{16}$$

where

$$T^{00} = (\epsilon + P)u^0u^0 - P\tag{17}$$

Their solutions on the computer yield the functions $T(x)$, $\lambda_g(x)$ and hence $n_g(x)$ subject to the stated initial conditions.

IV THERMALLY-AVERAGED RATE

Preliminaries: Next, we turn to the question of applying statistical mechanics to gluonic break-up of the J/ψ moving inside an expanding parton plasma. In the fireball

frame consider a ψ meson of mass m_ψ , four momentum $p_\psi = (p_\psi^0, \vec{p}_\psi)$, three velocity \vec{v}_ψ and dilation factor γ_ψ defined by

$$\vec{v}_\psi = \vec{p}_\psi/p_\psi^0, \quad \gamma_\psi = p_\psi^0/m_\psi = (1 - \vec{v}_\psi^2)^{-1/2} \quad (18)$$

The invariant quantum mechanical dissociation rate Γ for $g - \psi$ collision may be written compactly as

$$\Gamma = v_{\text{rel}} \sigma \quad (19)$$

where v_{rel} is the relative flux and σ the cross section measured in any chosen frame. Its thermal average over gluon momentum in the *fireball* frame reads

$$\langle \Gamma(x) \rangle = \frac{16}{n_g(x)} \int \frac{\widetilde{d^3K}}{(2\pi)^3} \Gamma f \quad (20)$$

Here the tilde implies that the gluon is hard enough to break J/ψ and the gluonic distribution function f is evaluated at the *location* of the ψ meson *viz.* at the time-space point

$$x = (t, \vec{x}_\psi) \quad (21)$$

The highly nontrivial integral (20) is best handled in the ψ meson rest frame by generating several useful kinematic informations as follows.

Kinematics in J/ψ Rest Frame: Let $q = (q^0, \vec{q})$ be the gluon 4 momentum measured in ψ meson *rest* frame. Since the relative flux becomes $v_{\text{rel}}^{\text{Rest}} = c = 1$ hence our invariant Γ reduces to the QCD [16] based cross section

$$\begin{aligned} \Gamma &= \sigma_{\text{Rest}} = B(Q^0 - 1)^{3/2}/Q^{05}; \quad q^0 \geq \epsilon_\psi \\ Q^0 &= \frac{q^0}{\epsilon_\psi} \geq 1; \quad B = \frac{2\pi}{3} \left(\frac{32}{3}\right)^2 \frac{1}{m_c(\epsilon_\psi m_c)^{1/2}} \end{aligned} \quad (22)$$

here ϵ_ψ is the J/ψ binding energy and m_c the charmed quark mass. This σ_{Rest} possesses a sharp peak at the gluon energy

$$q_p^0 = \frac{10\epsilon_\psi}{7} = 0.92 \text{ GeV}; \quad Q_p^0 = \frac{10}{7} \quad (23)$$

Also, the energy variable for the massless gluon transforms *via*

$$K^0 = \gamma_\psi (q^0 + \vec{v}_\psi \cdot \vec{q}) = \gamma_\psi q^0 (1 + |\vec{v}_\psi| \cos \theta_{q\psi}) \quad (24)$$

with $\theta_{q\psi}$ being the angle between \hat{q} and \hat{v}_ψ unit vectors. Furthermore, the fluid 4- velocity $w = (w^0, \vec{w})$ seen in ψ rest frame will be explicitly given by the Lorentz transformations

$$w^0 = \gamma_\psi (u^0 - \vec{u} \cdot \vec{v}_\psi) = \gamma_\psi \gamma (1 - \vec{v} \cdot \vec{v}_\psi) \quad (25)$$

$$\begin{aligned} \vec{w} &= \left[\vec{u} - (\vec{u} \cdot \hat{v}_\psi) \hat{v}_\psi \right] + \gamma_\psi \left[(\vec{u} \cdot \hat{v}_\psi) - u^0 |\vec{v}_\psi| \right] \hat{v}_\psi \\ &= \gamma \left[\vec{v} - \gamma_\psi \vec{v}_\psi + (\gamma_\psi - 1) (\vec{v} \cdot \hat{v}_\psi) \hat{v}_\psi \right] \end{aligned} \quad (26)$$

Finally, the scalar product

$$K \cdot u = q \cdot w = q^0 w^0 - q^0 |\vec{w}| \cos \theta_{qw} \quad (27)$$

where θ_{qw} is the angle between \hat{q} and \hat{w} . We thus have all the ingredients needed to calculate the thermally-averaged rate of (20).

Evaluation of $\langle \Gamma(x) \rangle$: Upon taking the polar axis for \vec{q} integration along \hat{v}_ψ , denoting the solid angle element by $d\Omega_{q\psi}$, and expanding f in a power series we can write

$$\langle \Gamma(x) \rangle = \frac{16}{n_g} \int \frac{d^3 q}{(2\pi)^3} \frac{K^0}{q^0} \sigma_{\text{Rest}} \sum_{n=1}^{\infty} \lambda_g^n e^{-nK \cdot u/T} \quad (28)$$

$$= \frac{2}{\pi^3 n_g} \int_{\epsilon_\psi}^{\infty} dq^0 q^{02} \int_0^{4\pi} d\Omega_{q\psi} \gamma_\psi (1 + |\vec{v}_\psi| \cos \theta_{q\psi}) \sigma_{\text{Rest}} \sum_{n=1}^{\infty} \lambda_g^n e^{-nq \cdot w/T} \quad (29)$$

This integral is performed in the Appendix based on the following nomenclature.

Symbols/Notations: Using the nomenclature in the fireball frame we define

$$\begin{aligned} (\theta_v, \phi_v) &= \text{polar angles of } \hat{v} ; (\theta_{v_\psi}, \phi_{v_\psi}) = \text{polar angles of } \hat{v}_\psi \\ F &= \vec{v} \cdot \hat{v}_\psi = |\vec{v}| \left[\sin \theta_v \sin \theta_{v_\psi} \cos(\phi_v - \phi_{v_\psi}) + \cos \theta_v \cos \theta_{v_\psi} \right] \\ Y &= \gamma_\psi |\vec{v}_\psi| - (\gamma_\psi - 1) F \\ w^0 &= \gamma \gamma_\psi (1 - F |\vec{v}_\psi|) ; \vec{w} = \gamma (\vec{v} - Y \hat{v}_\psi) \\ |\vec{w}| &= [|\vec{w}|^2]^{1/2} = \gamma \left[|\vec{v}|^2 + Y^2 - 2YF \right]^{1/2} \\ \theta_{\psi w} &= \text{angle between } \hat{v}_\psi \text{ and } \hat{w} \\ \cos \theta_{\psi w} &= \frac{1}{|\vec{w}|} (\vec{w} \cdot \hat{v}_\psi) = \frac{1}{|\vec{w}|} (F - Y) \end{aligned} \quad (30)$$

Also will be needed

$$\begin{aligned} Q^0 &= q^0 / \epsilon_\psi ; C_n = n \epsilon_\psi w^0 / T \\ D_n &= n \epsilon_\psi |\vec{w}| / T ; \rho_n = D_n Q^0 \end{aligned}$$

$$\begin{aligned}
A_n^\pm &= C_n \pm D_n = n\epsilon_\psi(w^0 \pm |\vec{w}|)/T \\
I_0(\rho_n) &= \sinh(\rho_n)/\rho_n \\
I_1(\rho_n) &= \cosh(\rho_n)/\rho_n - \sinh(\rho_n)/\rho_n^2 \\
nK \cdot u/T &= nq \cdot w/T = C_n Q^0 - \rho_n \cos \theta_{qw}
\end{aligned} \tag{31}$$

Result of Integration: From Appendix (A4) we find

$$\begin{aligned}
\langle \Gamma(x) \rangle &= \frac{8\epsilon_\psi^3 \gamma_\psi}{\pi^2 n_g} \sum_{n=1}^{\infty} \lambda_g^n \int_1^{\infty} dQ^0 Q^{02} \sigma_{\text{Rest}}(Q^0) e^{-C_n Q^0} \\
&\quad \times \left[I_0(\rho_n) + I_1(\rho_n) |\vec{v}_\psi| \cos \theta_{\psi w} \right]
\end{aligned} \tag{32}$$

By decomposing the hyperbolics I_0 and I_1 into exponentials this result can also be expressed as

$$\begin{aligned}
\langle \Gamma(x) \rangle &= \frac{4\epsilon_\psi^2 T \gamma_\psi}{\pi^2 |\vec{w}| n_g} \sum_{n=1}^{\infty} \frac{\lambda_g^n}{n} \int_1^{\infty} dQ^0 Q^0 \sigma_{\text{Rest}}(Q^0) \\
&\quad \times \left[\left(1 + \vec{v}_\psi \cdot \hat{w} (1 - 1/\rho_n) \right) e^{-A_n^- Q^0} \right. \\
&\quad \left. - \left(1 - \vec{v}_\psi \cdot \hat{w} (1 + 1/\rho_n) \right) e^{-A_n^+ Q^0} \right]
\end{aligned} \tag{33}$$

Remarks: The expressions (32, 33) are original and demonstrate how the mean dissociation rate $\langle \Gamma(x) \rangle$ depends on the *hydrodynamic* flow through $|\vec{w}|$ (or w^0) as well as the angle $\theta_{\psi w}$ in the notation of (30). The structure of $\exp(\pm D_n Q^0)$ tells that numerical treatment of (32) is convenient if $0 \leq |\vec{w}| \leq T/\epsilon_\psi$ while that of (33) is suitable if $T/\epsilon_\psi \leq |\vec{w}| \leq \infty$. From the analytical viewpoint it is much more advisable to work with the modified rate

$$\langle \tilde{\Gamma}(x) \rangle \equiv n_g(x) \langle \Gamma(x) \rangle \tag{34}$$

This is because $\langle \tilde{\Gamma} \rangle$ is devoid of any n_g factor appearing in the denominator of (32). Furthermore, $\langle \tilde{\Gamma} \rangle$ will be seen to enter directly the survival chance e^{-W} in (51) later.

Analytical estimate The physical interpretation of our graphs below will be facilitated by deriving a rough approximation for $\langle \tilde{\Gamma} \rangle$ as follows. In Eq.(32) we retain only the $n = 1$ term of the summation, and approximate the integrand by its peak value at Q_p^0 (cf.23) so that the desired estimate of (34) becomes

$$\begin{aligned}
\langle \tilde{\Gamma}(x) \rangle &\approx \frac{8\epsilon_\psi^3 \gamma_\psi}{\pi^2} \lambda_g \int_1^{\infty} dQ^0 Q^{02} \sigma_{\text{Rest}} H \\
&\propto \lambda_g \gamma_\psi H
\end{aligned} \tag{35}$$

Here the *entire* dependence on the flow velocity w is contained in the function

$$H \equiv e^{-C_1 Q_p^0} \left[I_0(D_1 Q_p^0) + I_1(D_1 Q_p^0) |\vec{v}_\psi| \cos \theta_{\psi w} \right] \quad (36)$$

with the coefficients C_1 , D_1 and A_1^\pm read-off from (31). We are now ready to discuss some consequences of (35) in *three* cases *viz.* static medium in the fireball frame, no flow in the J/ψ rest frame, and ultrarelativistic flow in either frame.

Static Medium in Fireball Frame: Remembering the notations (30, 31) consider the *hypothetical* case

$$\begin{aligned} \vec{v} &= \vec{0} ; \gamma = 1 ; F = 0 ; Y = \gamma_\psi |\vec{v}_\psi| \\ w^0 &= \gamma_\psi ; \vec{w} = -\gamma_\psi \vec{v}_\psi ; C_n = n \epsilon_\psi \gamma_\psi / T, \cos \theta_{\psi w} = -1 \\ D_n &= C_n |\vec{v}_\psi| ; A_n^\pm = C_n (1 \pm |\vec{v}_\psi|) \end{aligned} \quad (37)$$

This is precisely the case treated in our earlier paper [9] where the $g - \psi$ relative flux was correctly taken in the ψ meson rest frame. Eqs.(32, 33) also improve the work of Xu et al [8] who had written the $g - \psi$ relative flux in the fireball frame. Figs.1, 2 borrowed from Ref.[9] display the temperature and transverse momentum dependence of the *usual* rate $\langle \Gamma \rangle$ based on (32, 33) relevant to the LHC(1) initial fugacity λ_{gi} . For the sake of comparison the corresponding curves of the *modified* rate $\langle \tilde{\Gamma} \rangle$ using (34) are drawn in Figs.3, 4. Due to the assumed absence of flow there is no inhomogeneity with respect to x and the J/ψ formation time is also ignored at this stage. Various features of the indicated diagrams are interpreted in the next paragraph.

Interpretation i) Following the arguments given by Xu et al [8] it is known that the peak of σ_{Rest} at Q_p^0 gives a rich structure to the usual rate $\langle \Gamma \rangle$ in Figs 1, 2. ii) However, the modified rate $\langle \tilde{\Gamma} \rangle$ in Figs.3, 4 becomes structureless, i.e., monotonic. This is because the gluon number density n_g in (11) contains a crucial T^3 factor which changes from a low value *viz.* 0.008 at $T = 0.2$ GeV to a high value *viz.* 1.0 at $T = 1$ GeV. Such a T^3 coefficient matters a lot in the conversion of $\langle \Gamma \rangle$ to $\langle \tilde{\Gamma} \rangle$ *via* (34). iii) At fixed p_T the steady *increase* of $\langle \tilde{\Gamma} \rangle$ with T in Fig. 3 is caused by the growing $\exp(-A_1^\pm Q_p^0)$ factors of the estimate (35, 36). iv) At fixed T the monotonic *decrease* of $\langle \tilde{\Gamma} \rangle$ with p_T in Fig. 4 has a very interesting explanation. For the situation (37) under study $\vec{w} = -\gamma_\psi \vec{v}_\psi$ is antiparallel to \vec{v}_ψ so that $\cos \theta_{\psi w} = -1$. Hence partial wave terms I_0 and I_1 of H (36) *interfere* destructively in Fig. 4 making $\langle \tilde{\Gamma} \rangle$ small as $|\vec{v}_\psi|$ grows.

No Flow in J/ψ Rest Frame: Next, consider a configuration in the fireball frame such that the 3 velocities of the plasma and ψ meson coincide at some x . This is

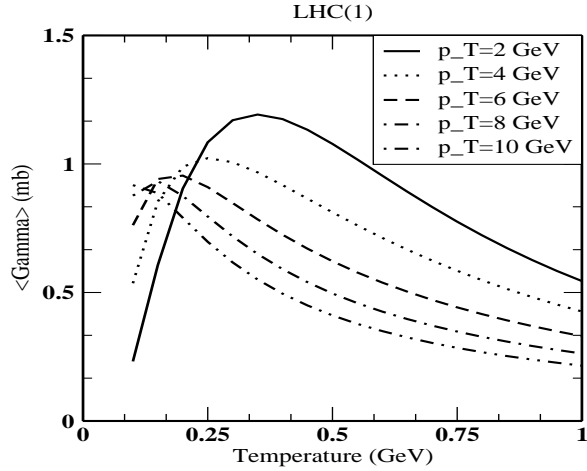


Figure 1: The thermal-averaged gluon- ψ dissociation cross section $\langle \Gamma \rangle \equiv \langle v_{\text{rel}} \sigma \rangle$ as a function of temperature at different transverse momenta p_T as in [9, Eq.(19)], i.e., in the absence of longitudinal flow. The initial gluon fugacity is given in Table 1 at LHC energy.

possible if, for example, both the fluid and ψ are moving in the transverse direction. Then in (30, 31) we put

$$\begin{aligned} \vec{v} &= \vec{v}_\psi ; F = |\vec{v}_\psi| ; w^0 = 1 ; \vec{w} = \vec{0} \\ C_n &= n\epsilon_\psi/T ; \rho_n = 0 ; I_0(\rho_n) = 1 ; I_1(\rho_n) = 0 \end{aligned} \quad (38)$$

Inserting this information into the exact formulae (32, 34) and attaching a suffix 0 we find

$$\langle \tilde{\Gamma}(x) \rangle_0 = \frac{8\epsilon_\psi^3 \gamma_\psi}{\pi^2} \sum_{n=1}^{\infty} \lambda_g^n e^{-n\epsilon_\psi/T} \int_1^{\infty} dQ^0 Q^{02} \sigma_{\text{Rest}} \quad (39)$$

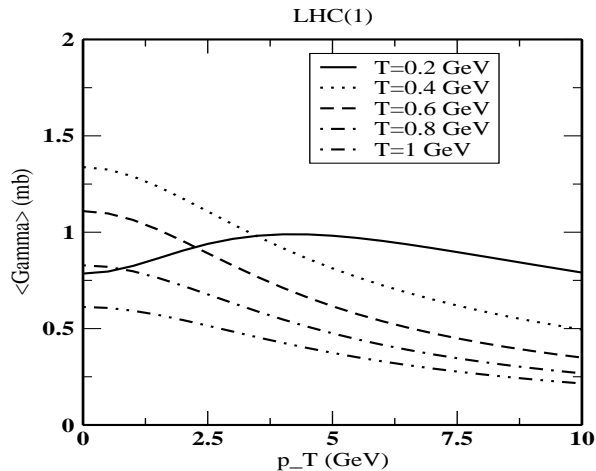


Figure 2: The variation of $\langle \Gamma \rangle \equiv \langle v_{\text{rel}} \sigma \rangle$ with transverse momentum at different temperatures [9] as in Fig.1 in absence of flow profile.

Its variations with T and p_T are displayed in Figs.5, 6 relevant to the LHC(1) initial fugacity. The crude proportionality (35) now reduces to

$$\langle \tilde{\Gamma}(x) \rangle_0 \propto \lambda_g \gamma_\psi e^{-\epsilon_\psi/T} \quad (40)$$

which is utilized below to explain some features of the graphs.

Interpretation i) At fixed p_T our $\langle \tilde{\Gamma}(x) \rangle_0$ of Fig.5 rises monotonically with T in analogy with the earlier Fig.3. This is caused by the $e^{-\epsilon_\psi/T}$ factor present in the estimate (40). ii) At fixed T our $\langle \tilde{\Gamma}(x) \rangle_0$ of Fig.6 grows steadily with p_T in contrast to the earlier Fig.4. Such a behaviour is due to the coefficient γ_ψ occurring in (40). iii) The curves of Figs.5, 6 are consistently *higher* than those of Figs.3, 4. The reason is that there is no $I_1(\rho_n)$ term present in (39) to interfere destructively with the $I_0(\rho_n)$ term in view of the restriction (38).

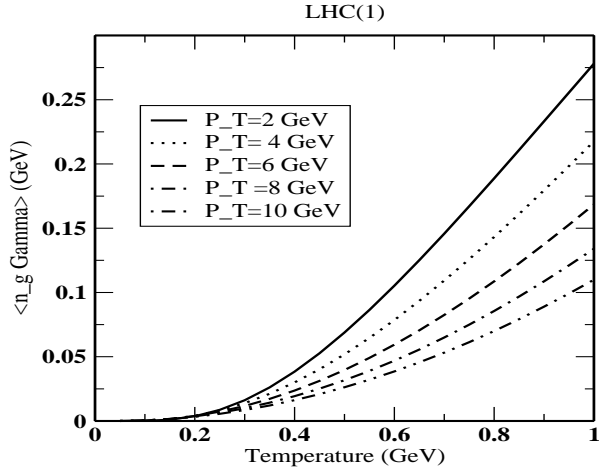


Figure 3: The variation of the *modified rate* $\langle \tilde{\Gamma} \rangle \equiv n_g \langle \Gamma \rangle$ with temperature at different values of transverse momentum corresponding to $\langle \Gamma \rangle$ of Fig.1 is depicted here.

Ultrarelativistic Flow in Either Frame: Finally, suppose at a point x in the fireball frame the medium is flowing ultrarelativistically ($|\vec{v}| \rightarrow 1$) and the J/ψ is moving slowly ($|\vec{v}_\psi| < 1/10$, say). In the ψ meson rest frame the Lorentz transformation (26) shows that \vec{w} almost equals $\gamma\vec{v}$ so that $\cos \theta_{\psi w} \rightarrow \hat{v}_\psi \cdot \hat{v}$. [Hence, in the case of pure transverse expansion of the plasma $\cos \theta_{\psi w}$ can even become +1 implying a constructive interference between the I_0 and I_1 terms of (36); this possibility will, however, be discussed in a future communication. At present, we illustrate the case of both the J/ψ and plasma moving ultrarelativistically (in the transverse and longitudinal directions, respectively) subject to the following kinematic conditions:

$$\begin{aligned} \vec{v} &= 0.9 \hat{e}_z; \quad \gamma = 2.3; \quad F = 0; \quad Y = \gamma_\psi |\vec{v}_\psi| \\ w^0 &= \gamma\gamma_\psi \gg 1; \quad |\vec{w}| \approx \gamma\gamma_\psi - \frac{1}{2\gamma\gamma_\psi} \end{aligned}$$

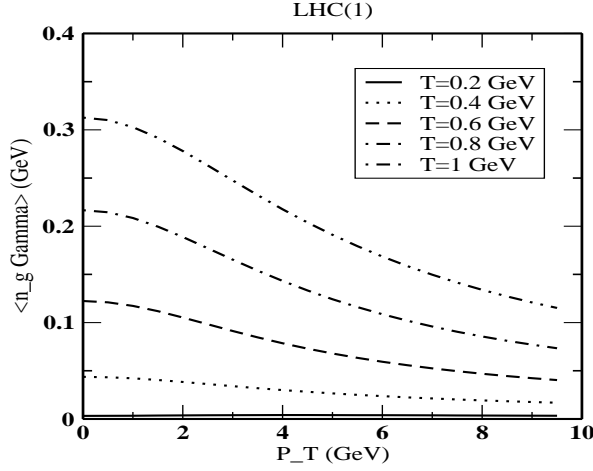


Figure 4: The variation of the *modified rate* $\langle \tilde{\Gamma} \rangle \equiv n_g \langle \Gamma \rangle$ with transverse momentum at different values of temperatures corresponding to $\langle \Gamma \rangle$ of Fig.2 is shown here in absence of flow.

$$\cos \theta_{\psi w} = -\frac{Y}{|\vec{w}|} \approx -\frac{1}{\gamma}; \quad D_1 = \epsilon_\psi |\vec{w}|/T \sim \frac{\epsilon_\psi \gamma \gamma_\psi}{T} \gg 1$$

$$A_1^- = \frac{\epsilon_\psi}{T} (w^0 - |\vec{w}|) \approx \frac{\epsilon_\psi}{2T \gamma \gamma_\psi} \quad (41)$$

Then $I_o(\rho_1) \rightarrow I_1(\rho_1) \rightarrow \exp(\rho_1)/2\rho_1$ so that our rough estimate (35, 36) become

$$\langle \tilde{\Gamma}(x) \rangle \propto \frac{\lambda_g T}{\gamma} \exp\left(-\frac{\epsilon_\psi Q_p^0}{2T \gamma \gamma_\psi}\right) \left[1 - \frac{|\vec{v}_\psi|^2}{\gamma}\right] \quad (42)$$

This information will be utilized below for explaining the main features of the graphs.

Interpretation i) For fixed p_T , v the exponential in (42) tend to 0 as $T \rightarrow 0$ and tends to 1 as $T \rightarrow \infty$. Therefore, the growing trend of $\langle \tilde{\Gamma}(x) \rangle$ with T in Fig. 7 is

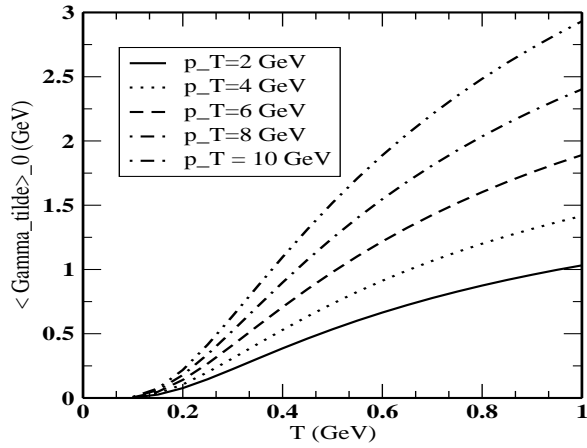


Figure 5: The variation of the *modified* rate $\langle \tilde{\Gamma}(x) \rangle_0$ from Eq.(39) with temperature for different p_T 's, when the 3 fluid velocity \vec{w} in the ψ meson rest frame is zero.

understable. ii) At fixed T , v the rich behaviour of $\langle \tilde{\Gamma}(x) \rangle$ with p_T in Fig. 8 arises from a sensitive competition between the bracketed factors of (42). iii) More precisely, at lower temperatures $T, \leq 0.4$ GeV the exponential factor in (42) increases dominantly with p_T causing $\langle \tilde{\Gamma}(x) \rangle$ to grow. iv) But at higher temperatures $T \geq 0.8$ GeV the third bracket in (42) decreases prominently with p_T causing $\langle \tilde{\Gamma} \rangle$ to drop. v) Comparison of Figs.(3,4) with Figs.(7,8) tells that the p_T - dependence of $\langle \tilde{\Gamma} \rangle$ (unlike its T dependence) is quite sensitive to the nonrelativistic/ultrarelativistic nature of flow in the fireball frame.

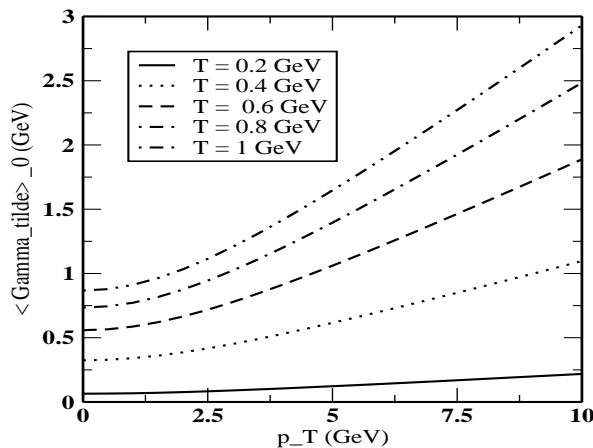


Figure 6: The variation of the *modified* rate $\langle \tilde{\Gamma}(x) \rangle_0$ from Eq. (39) with p_T 's for different values of T 's when the 3 fluid velocity \vec{w} in the ψ meson rest frame is zero.

V J/ψ SURVIVAL PROBABILITY

Next, we ask the important question as to how the explicit collective flow profile affects the birth and death scenarios of ψ mesons within a quark gluon plasma? Below we consider only *longitudinal* expansion; the case of transverse flow will be dealt with in a future communication.

Pure Longitudinal Expansion: Suppose at general instant t in the fireball frame the plasma is contained inside a *cylinder* of radius R , cross section $A = \pi R^2$, length L , and volume $V = AL$. Keeping the origin at its centre and assuming constant speed of longitudinal expansion we have

$$R = R_i, \quad A = A_i, \quad L = L_i t / t_i, \quad V = V_i t / t_i \quad (43)$$

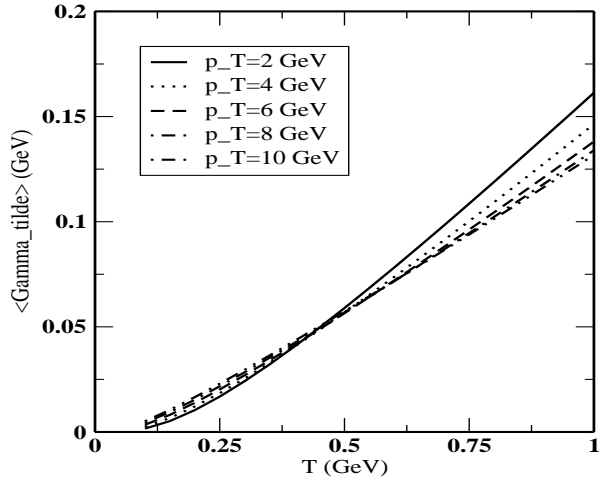


Figure 7: The variation of the *modified rate* $\langle \tilde{\Gamma}(x) \rangle$ using Eqs.(32, 34) as a function of temperature at different transverse momenta for the ultrarelativistic longitudinal flow velocity $v = 0.9 c$.

where the suffix i labels *initial* values. The ansatz (4) of the velocity profile reads

$$\vec{v} = z\hat{e}_z/t ; \quad -L/2 \leq z \leq +L/2 \quad (44)$$

subject to the restriction that the speed at the edges $\pm L/2$ must be less than c , i.e.,

$$\frac{L}{2t} = \frac{L_i}{2t_i} < 1 \quad (45)$$

Production configuration of J/ψ : Employing cylindrical coordinates let a typical ψ meson be created at the instant t_I , having position \vec{x}_ψ^I , and with transverse velocity \vec{v}_ψ^I (in the mid-rapidity region) such that

$$t_I = t_i + \gamma_\psi \tau_F ; \quad \vec{x}_\psi^I = (\vec{r}_\psi^I, z_\psi^I) = (r_\psi^I, \phi_\psi^I, z_\psi^I)$$

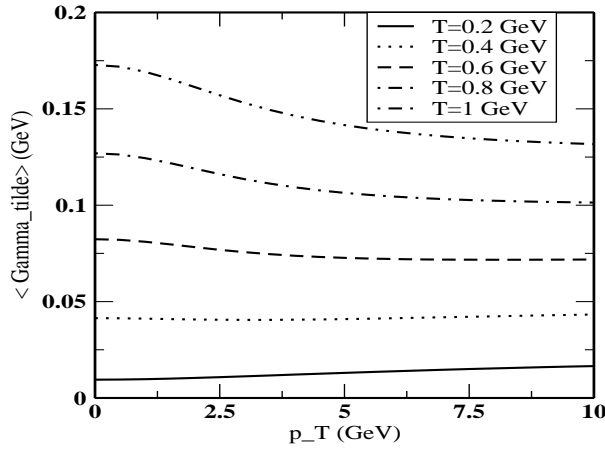


Figure 8: The variation of the *modified* rate $\langle \tilde{\Gamma}(x) \rangle$ using Eqs.(32, 34) as a function of p_T at different values of temperatures as in Fig.7 corresponding to ultrarelativistic longitudinal flow velocity $v = 0.9 c$.

$$\begin{aligned} \vec{v}_\psi^I &= \vec{v}_\psi = (\vec{v}_\psi^T, 0) = (v_T, 0, 0) \\ F &= \vec{v} \cdot \hat{v}_\psi = (z\hat{e}_z/t) \cdot \hat{v}_\psi^T = 0 \end{aligned} \quad (46)$$

where $\tau_F \approx 0.89$ fm/c is the *formation* time of the bound state in the $c\bar{c}$ barycentric frame. Of course, the concept of formation time was not utilized while drawing the graphs 1-8 in Sec.IV.

Kinematics of J/ψ Trajectory: The position 3 vector at general instant t becomes

$$\vec{x}_\psi \equiv [\vec{r}_\psi, z_\psi] = [\vec{r}_\psi^I + (t - t_I)\vec{v}_\psi^T, z_\psi^I] \quad (47)$$

The transverse trajectory will hit the cylinder of radius $R = R_I$ after a time interval t_{RI}

by covering a distance d_{RI} such that

$$\begin{aligned} |\vec{r}_\psi^I + t_{RI} \vec{v}_\psi^I| &= R_I ; t_{RI} = d_{RI}/v_T \\ d_{RI} &= -r_\psi^I \cos \phi_\psi^I + \sqrt{R_I^2 - r_\psi^{I2} \sin^2 \phi_\psi^I} \end{aligned} \quad (48)$$

In the fireball frame the full temporal range of our interest is obviously

$$t_I \leq t \leq t_{II} ; t_{II} = \min(t_I + t_{RI}, t_{\text{life}}) \quad (49)$$

This prescription was also utilized in [9] and it improves the work of [8] by incorporating the formation time.

Formulation of $S(p_T)$: Let us return to the modified dissociation rate derived in Sec.IV. The value $F = 0$ (cf.(46)) greatly simplifies the kinematics of (30). Furthermore, since the time-space point x in (21) is to be chosen on the J/ψ trajectory itself hence the notation $\langle \tilde{\Gamma}(x) \rangle$ of (34) is equivalent to

$$\langle \tilde{\Gamma}[t] \rangle \equiv \langle \tilde{\Gamma}(t, p_T, z_\psi^I) \rangle \quad (50)$$

This depends parametrically on z_ψ^I in view of the longitudinal flow profile (44), and the upper limit t_{II} (cf. (49)) of the time variable depends on the production configuration r_ψ^I, ϕ_ψ^I . Then by the law of radioactive decay without recombination the effective survival chance of a chosen ψ meson will be given by the exponential e^{-W} with

$$W = \int_{t_I}^{t_{II}} dt n_g[t] \langle \tilde{\Gamma}[t] \rangle \quad (51)$$

Upon averaging e^{-W} over the production configuration of the ψ 's we arrive at the final expression for the net survival probability

$$\begin{aligned} S(p_T) &= \int_{V_I} d^3x_\psi^I (R_I^2 - r_\psi^{I2}) e^{-W} / \int_{V_I} d^3x_\psi^I (R_I^2 - r_\psi^{I2}) \\ d^3x_\psi^I &= dr_\psi^I r_\psi^I d\phi_\psi^I dz_\psi^I \end{aligned} \quad (52)$$

Remarks: This is a new result showing that due to the inhomogeneity introduced by the ensuing longitudinal expansion the spatial integration in (52) must extend over the volume $V_I = V_i t_I / t_i$ available at the instant of creation. Hence the entry concerning the initial length L_i and radius R_i of the plasma becomes essential in Table 2. However, in the absence of collective flow the integral needs to run only over the cross sectional area A_I of the fireball as was done in Refs [9, 8].

Table 2: Colliding nuclei, collision energy, initial length of cylindrical QGP, and its radius at RHIC(1) and LHC(1). The length is assumed to lie in the range $0.1 \leq L_i \leq 1$ fm since the sea-quarks of the nucleon are spread over a distance of order $\Lambda \approx 1$ fm. [We do not use the L_i corresponding to directly Lorentz-contracted, disc-shaped nuclei to avoid too large or too small values.]

	Nuclei	Energy(\sqrt{s}) (GeV/nucleon)	L_i (fm)	R_i (fm)
RHIC(1)	Au^{197}	200	$0.1 \leq L_i \leq 1$	6.98
LHC(1)	Pb^{208}	5000	$0.1 \leq L_i \leq 1$	7.01

Numerical Illustration: As pointed out in Ref. [9] the precise value of the ψ meson formation time τ_F is ambiguous; however we adopt $\tau_F \simeq 0.89$ fm/c as a fair representative. For chosen creation configuration of the ψ meson the function W was first computed from (51) and then the survival probability was numerically evaluated using (52). Figs 9 and 10 show the dependence of $S(p_T)$ on the transverse momentum corresponding to the LHC(1) and RHIC(1) initial conditions, respectively (cf. Tables 1, 2). The dotted ($L_i = 0.1$ fm) and dashed ($L_i = 1$ fm) curves are computed in the *presence* of longitudinal flow while the solid curve is borrowed from [9] in the *absence* of hydrodynamic flow profile. The main features of these graphs may be explained as follows.

Interpretation i) In the absence of flow, i.e., for $v = 0$, the $S(p_T)$ solid lines in Figs.9, 10 rise steadily with p_T . This is because $\langle \tilde{\Gamma} \rangle$ of Fig.4, and hence the W integral of (51), diminish with p_T . ii) In the presence of flow with small initial length $L_i \sim 0.1$ fm the $S(p_T)$ dotted curves in Figs.9, 10 are slightly above the solid line. To explain this we note that the flow profile $v = z/t$ remains nonrelativistic over short lengths and the destructive interference between I_0 and I_1 terms in (36) becomes slightly stronger (compared to the $v = 0$ case). The consequent drop of $\langle \tilde{\Gamma} \rangle$ or W pushes $S(p_T)$ upwards. iii) In the presence of flow with large initial length $L_i = 1$ fm the $S(p_T)$ dashed curve lies below the solid line in the LHC case (cf. Fig.9) but lies above the solid line in RHIC case (cf. Fig. 10). iv) To explain this peculiar contrast between Figs. 9 and 10 we note that as the expanding cylinder becomes much bigger than 1 fm the flow profile $v = z/t$ may become relativistic over its substantial length so that the graphs of Fig.8

can be employed. At higher temperatures ($0.8 < T < 0.6$, say) at LHC the $\langle \tilde{\Gamma} \rangle$ curves are known to drop with increasing p_T . But at lower temperatures ($0.6 < T < .2$), say) at RHIC the $\langle \tilde{\Gamma} \rangle$ curves rise with p_T in Fig.8 whereby a contrast occurs. v) Of course, the relative shift in $S(p_T)$ due to longitudinal flow is only about 10% to 15% even at $p_T = 10$ GeV.

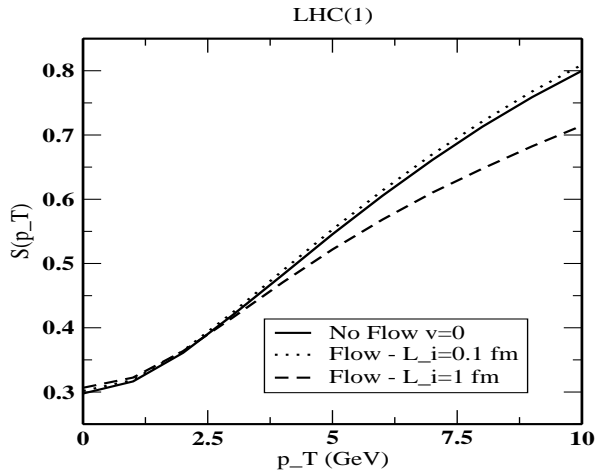


Figure 9: The survival probability of J/ψ in an equilibrating parton plasma at LHC energy with initial conditions given in Table 1. The solid curve is the result of Ref. [9], i.e., in the *absence of flow* while the dotted and dashed curves represent the survival of J/ψ when the plasma is undergoing longitudinal expansion with the initial values of the length of the cylinder $L_i = 0.1$ fm and 1 fm, respectively.

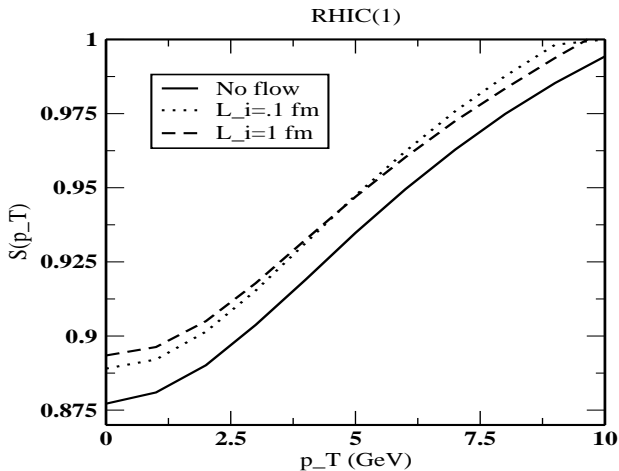


Figure 10: Same as Fig.9 but computed for RHIC initial conditions.

VI Conclusions

(a) In this paper we have extended our earlier work [9] by explicitly including the effect of hydrodynamic expansion profile on the gluonic dissociation of J/ψ 's created in an equilibrating QGP. The treatment of Secs.III and IV is very general in the sense that both the fluid velocity \vec{v} and ψ momentum \vec{p}_ψ are arbitrary. Only in Sec.V we specialize to longitudinal fluid expansion and transverse motion of ψ .

(b) Our theoretical formulae for the gluon number density n_g (cf.11), modified $g - \psi$ breakup rate $\langle \tilde{\Gamma} \rangle$ (cf.34), and ψ survival probability S (cf.52) are new. These are derived by making careful Lorentz transformations between the rest frames of the fireball, plasma, and ψ meson.

(c) At specified fugacity λ_g the effect of the flow velocity \vec{v} is to increase the number density of hard gluons (which are primarily responsible for breaking the J/ψ 's) as shown in the numerical estimate (12).

(d) Our expression (32, 34) of $\langle \tilde{\Gamma}(x) \rangle$ contains partial wave contributions called I_0 and I_1 whose mutual interference is controlled by the anisotropic $\cos\theta_{\psi w}$ factor. This significantly affects the variation of $\langle \tilde{\Gamma} \rangle$ with T , p_T and \vec{v} as depicted in Figs. 3-8.

(e) The presence of longitudinal expansion pushes up the graph of $S(p_T)$ compared to the $v \equiv 0$ case for nonrelativistic flow appropriate to small initial length $L_i = 0.1\text{fm}$.

(f) However, in the case of relativistic longitudinal flow appropriate to larger initial length $L_i = 1\text{fm}$ the downward shift of $S(p_T)$ graph at LHC is in sharp contrast to the upward shift at RHIC. Such a contrast between the behaviours at LHC and RHIC is caused by the different initial temperatures generated therein. The relative shift is, however, is only 10% - 15% even at $p_T = 10\text{ GeV}$.

(g) In a future communication we plan to study the detailed effect of transverse expansion of the medium on $S(p_T)$. It is expected that there will be a more rapid cooling with time and also a possible constructive interference in (35).

ACKNOWLEDGEMENTS

VJM thanks the UGC, Government of India, New Delhi for financial support. We thank Dr. Dinesh Kumar Srivastava for useful discussions during this work.

References

- [1] Helmut Satz, Rept.Prog.Phys. **63**, 1511 (2000).
- [2] T. Matsui and H. Satz, Phys. Lett. B **178**, 416 (1986).
- [3] B. K. Patra, D. K. Srivastava, Phys. Lett. B **505**, 113 (2001).
- [4] D. Kharzeev and H. Satz, Phys. Lett. B **334**, 155 (1994).
- [5] D. Kharzeev and H. Satz, Phys. Lett B **366**, 316 (1996).

- [6] B. K. Patra and V. J. Menon, Nucl. Phys. A **708**, 353 (2002).
- [7] R. L. Thews, M. Schroedter, and J. Rafelski, Phys. Rev. C **63**, 054905 (2001).
- [8] Xiao-Ming Xu, D. Kharzeev, H. Satz, and Xin-Nian Wang, Phys. Rev. C **53**, 3051 (1996).
- [9] B. K. Patra and V. J. Menon, J/ψ -gluonic dissociation revisited:I. Fugacity, flux, and formation time effects, Eur. Phys. J. C **37**, 115 (2004).
- [10] T. S. Biro, E. van Doorn, M. H. Thoma, B. Müller, and X.-N. Wang, Phys. Rev. C **48**, 1275 (1993).
- [11] D. K. Srivastava, M. G. Mustafa, and B. Müller, Phys. Rev. C **56**, 1064 (1997).
- [12] D. Pal, B. K. Patra, and D. K. Srivastava, Eur. Phys. Jour. C **17**, 179 (2000).
- [13] Jean-Yves Ollitrault, Phys. Rev. D **46**, 229 (1992).
- [14] Xin-Nian Wang, Feng Yuan, Phys. Lett. B **540**, 62 (2002).
- [15] X.-N Wang and M. Gyulassy, Phys. Rev. D **44**, 3501 (1991).
- [16] M. E. Peskin, Nucl. Phys. B **156**, 365 (1979); G. Bhanot and M. E. Peskin, Nucl. Phys. B **156**, 391 (1979).
- [17] C. Gerschel and J. Hüfner, Phys. Lett. B **207**, 253 (1988).

Appendix

EVALUATION OF THE INTEGRAL (28)

Our derivation proceeds through the following steps :

First Step We recall the symbols (30, 31), work in the ψ meson rest frame, and rewrite (29) as

$$\begin{aligned} \langle \Gamma(x) \rangle &= \frac{2}{\pi^3 n_g} \int_1^\infty \epsilon_\psi^3 dQ^0 Q^{02} \int_0^{4\pi} d\Omega_{q\psi} \gamma_\psi \left[1 + |\vec{v}_\psi| \cos \theta_{q\psi} \right] \\ &\quad \times \sigma_{\text{Rest}} \sum_{n=1}^\infty \lambda_g^n e^{-C_n Q^0 + \rho_n \cos \theta_{qw}} \end{aligned} \quad (\text{A } 1)$$

Second step Next, a partial wave expansion is done of the exponential

$$\begin{aligned} e^{\rho_n \cos \theta_{qw}} &= \sum_{l=0}^\infty i^l j_l(-i\rho_n) (2l+1) P_l(\cos \theta_{qw}) \\ &= \sum_{l=0}^\infty I_l(\rho_n) 4\pi \sum_{m=-l}^l Y_l^{m*}(\Omega_{q\psi}) Y_l^m(\Omega_{\psi w}) \end{aligned} \quad (\text{A } 2)$$

Here $\rho_n = D_n Q^0$ as before, j_l denotes spherical Bessel functions, $I_l(\rho_n) = i^l j_l(-i\rho_n)$, the addition theorem has been used for the Legendre polynomial $P_l(\cos \theta_{qw})$, and $\Omega_{\psi w}$ are the polar angles of \hat{v}_ψ with respect to the local flow direction \hat{w} .

Third step Next, the relevant angular integral appearing in (A1,2) reads

$$\begin{aligned} \int_0^{4\pi} d\Omega_{q\psi} \left[1 + |\vec{v}_\psi| \cos \theta_{q\psi} \right] Y_l^{m*}(\Omega_{q\psi}) \\ = \sqrt{4\pi} \left[\delta_{l0} + \sqrt{\frac{1}{3}} |\vec{v}_\psi| \delta_{l1} \right] \delta_{m0} \end{aligned} \quad (\text{A } 3)$$

due to the orthogonality of spherical harmonics.

Fourth step Finally, inserting the informations (A2,3) back into the starting expression (A1) we obtain

$$\begin{aligned} \langle \Gamma(x) \rangle &= \frac{2}{\pi^3 n_g} \int_1^\infty \epsilon_\psi^3 dQ^0 Q^{02} \gamma_\psi \sigma_{\text{Rest}} \sum_{n=1}^\infty \lambda_g^n e^{-c_n Q^0} \\ &\quad 4\pi \sum_{l=0}^\infty I_l(\rho_n) \left[\delta_{l0} + \sqrt{\frac{1}{3}} |\vec{v}_\psi| \delta_{l1} \right] \sqrt{4\pi} Y_l^0(\Omega_{\psi w}) \end{aligned} \quad (\text{A } 4)$$

which indeed coincides with (32) of the text.